

# Cell-type Selective Stimulation of Neurons Based on Single Neuron Models

Manu Gopakumar, Jiaming Cao, Shawn K Kelly, and Pulkit Grover  
Carnegie Mellon University, Pittsburgh, United States  
{mgopakum, jiamingc, skkelly, pgrover}@andrew.cmu.edu

**Abstract**— Selectively stimulating neuron types within the brain can enable new treatment possibilities for neurological disorders and feedback in brain-machine interfaces. Prior computational work has shown that by choosing a sinusoidal signal with appropriate amplitude and frequency, one can obtain one-directional stimulation, i.e., one can stimulate a mammalian inhibitory neuron without stimulating an excitatory neuron. However, bidirectional selectivity is not achievable using just sinusoidal inputs. In this work, which is also computational, we design novel current waveforms to achieve this bidirectional selectivity. To do so, we explicitly exploit the non-linearity of neuronal membrane potential in response to stimulating currents. These current waveforms are able to stimulate either of the two neuron-types without stimulating the other. Further, we are also able to design a waveform which stimulates both neurons. Moreover, we can ensure a relatively high firing rate ( $\sim 100$  Hz) when a neuron-type is targeted for stimulation.

## I. INTRODUCTION

Selective stimulation of neurons based on neuron-type can greatly enhance the effectiveness of targeted stimulation techniques and treatment methods. Although techniques to perform electrical stimulation with spatial localization have been developed both invasively and noninvasively [1], [2], current-stimulation typically lacks neuron-type specificity. Work towards selective stimulation of neurons based on neuron-type is already ongoing. Freeman et al. [3] use different frequencies of sinusoidal signals to selectively simulate photoreceptors, bipolar cells, and ganglion cells. Similarly, Im and Fried [4] show that different frequencies of input could be used to selectively stimulate ON and OFF brisk transient retinal ganglion cells (RGCs). However, in these cases, selective stimulation can only be achieved at a different range of frequencies for each cell type since frequency is the only variable used to change the target for stimulation. Bidirectional selective stimulation cannot be achieved at the same high frequency using this method.

Limiting stimulation waveforms to sinusoids and viewing neural firing rate as a “transfer function,” while a dominant perspective in the literature, is fundamentally a linear perspective. This leaves unexplored a more general class of signals that can exploit the well known nonlinearity of the neural membrane potential as a function of the driving current. In a few works, a broader class of signals is examined. E.g., Twyford et al. [5] use modulated high frequency signals to achieve bidirectional stimulation between ON and OFF brisk transient RGCs. However, this method falls short of “clean” bidirectional stimulation: the selectivity simply increases the firing

rate of one neuron type over the other, but does not ensure the undesired neuron does not fire.

In this work, our goal is to develop strategies for performing bidirectional selective stimulation of two neuron-types by studying the non-linear dynamics of neural models, and validating them using computational neuron models. The benchmark for our work is the work of Mahmud and Vassanelli [6], who use models of the same neurons we use. Through variation of frequency and amplitude of sinusoidal inputs, they show that the inhibitory neuron can be stimulated without engagement of the excitatory neuron. However, no bidirectional selectivity is shown in [6]. Our novel waveforms utilize differences in the parameters of excitatory and inhibitory neurons, and obtain “clean” bidirectional stimulation (i.e. the firing rate of the non-targeted neuron is zero).

In Section II, we define our models for mammalian excitatory and inhibitory neurons and highlight key values differentiating the neuron types which govern the non-linear responses of the neurons. Then in Section III, we detail how signals can be crafted to take advantage of the differences and create bidirectional selective stimulation between the models. We demonstrate the flexibility of our strategies by showing that we can stimulate both neuron-types simultaneously, or selectively stimulate either of the neuron-types without engagement of the other.

## II. METHODS

### A. Neural Models and the Differences in Cell Dynamics

For demonstrating our selective stimulation strategies, we use Hodgkin-Huxley (HH)-style models to simulate the membrane potential of neurons in response to external currents. The original squid giant axon model [7] has, over the years, been adapted to represent other neuron-types. In our work, we adopt models that are calibrated against mammalian cortical neurons, namely an excitatory (pyramidal) neuron and an inhibitory neuron. For simplicity, we consider only isolated neurons, i.e. we do not model the effects of the neural network.

To most clearly demonstrate the utility of our techniques, we provide strategies that strictly and significantly improve on existing literature. Specifically, we utilize the same models used in an earlier computational study of Mahmud and Vassanelli [6]. There, as well as here, the excitatory neuron model is based on [8] with an additional leakage channel whose parameters are from [9], and the inhibitory neuron model is from [10].

Thus, for the same neuron models, our nonsinusoidal waveforms are able to obtain bidirectional selectivity, while sinusoidal waveforms in [6] only obtain unidirectional selectivity. In doing so, we exploit the understanding of the nonlinear dynamics of the neural membrane of the two neuron-types. These dynamics are described by equations given in (1) and (2) (below) respectively, where  $V$  denotes the membrane potential,  $C$  denotes the membrane capacitance,  $i$  denotes the external current input,  $E_X$  are the reverse potentials, and  $\bar{g}_X$  are the maximum possible conductances of the channels. In practice, the external current input would be set by manipulating the activating function of the neuron [12]. The detailed equations as well as values chosen for the constants can be found in Section IV.

$$\begin{aligned} \frac{dV}{dt} = & -\frac{1}{C} \left( \bar{g}_{Na} m^3 h \times (V - E_{Na}) + \bar{g}_K n^4 \times (V - E_K) \right. \\ & \left. + \bar{g}_L \times (V - E_L) \right) + \frac{i}{C} \end{aligned} \quad (1)$$

$$\begin{aligned} \frac{dm}{dt} = & \alpha_m(1-m) - \beta_m m; & \frac{dn}{dt} = & \alpha_n(1-n) - \beta_n n \\ \frac{dh}{dt} = & (\alpha_h + \beta_h)(h_\infty - h) \end{aligned}$$

$$\begin{aligned} \frac{dV}{dt} = & -\frac{1}{C} \left( \bar{g}_{Na} m^3 h \times (V - E_{Na}) + \bar{g}_K n^4 \times (V - E_K) \right. \\ & \left. + \bar{g}_L \times (V - E_L) \right) + \frac{i}{C} \end{aligned} \quad (2)$$

$$m_\infty = \frac{\alpha_m}{\alpha_m + \beta_m}; \quad \frac{dn}{dt} = 5(\alpha_n(1-n) - \beta_n n)$$

$$\frac{dh}{dt} = 5(\alpha_h(1-h) - \beta_h h).$$

Here,  $m$ ,  $n$ , and  $h$  are variables related to the opening probabilities of sodium activation, potassium activation, and sodium deactivation gates respectively, whose steady-state values as a function of membrane potential are given in Fig. 1. In addition to the differences in the steady-state values, what further enables selective stimulation is the differences in their time constants, i.e.  $m$ ,  $n$ ,  $h$  parameters in the two neuron-types approach their steady-state values at different speeds. The rather large differences of the time constants are illustrated in Fig. 2. Note that  $m$  in the inhibitory neuron model is modeled as instantaneous [10] so the time constant is always zero. For the rest of the paper, we aim to leverage such differences in the dynamics of the two neurons to design strategies for bidirectional selective stimulation.

### B. Selective Stimulation by Leveraging the Differences in Cell Dynamics

Examining Fig. 1 and Fig. 2 provides an understanding of the firing characteristics of neurons that is used to design selective stimulation strategies. First, we observe the behavior of the cell parameters as the neurons fire. We can see that the membrane potential of the neuron grows rapidly when  $m$  and  $h$  are high values due to

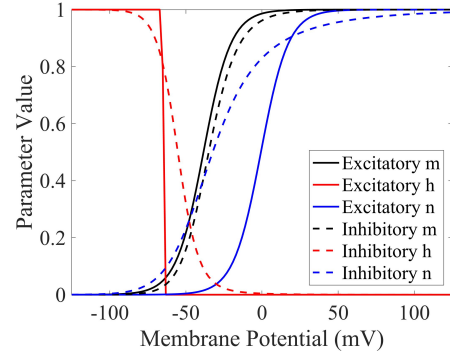


Fig. 1. Steady-state values for  $m$ ,  $n$ , and  $h$  plotted with respect to membrane potential.

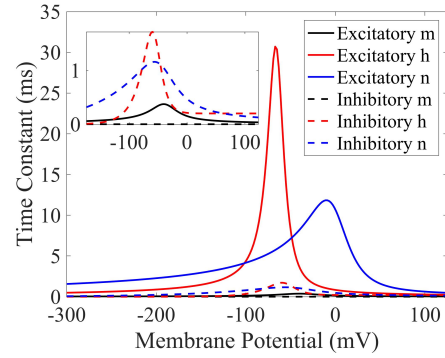


Fig. 2. Time constant values for  $m$ ,  $n$ , and  $h$  plotted with respect to membrane potential with zoomed view of low amplitude time constants. Note: The excitatory neuron is much slower than the inhibitory neuron.

the presence of  $m^3 h$  in the differential equation for the potential. The  $n^4$  in the equation contributes more to neuron recovery than neuron spike initiation. As a result, our focus is primarily on manipulating  $m^3 h$ . Thus, we can build the intuition that in order to stimulate a firing response in a neuron, from a resting state at which  $m$  is low and  $h$  is high, an input signal should increase the value of  $m$  sufficiently before the value of  $h$  decreases significantly. This is possible because the  $m$  parameter has a much lower time constant compared to  $h$ , so it responds to changes in the membrane potential more quickly than the  $h$  parameter responds. Additionally, for the different neuron models, the parameters have different time constants and steady-state values. As is shown in Fig. 2, the excitatory neuron is significantly slower than the inhibitory neuron, giving us an opportunity to leverage the different time constants to achieve selective stimulation. Intuitively, when the neurons are in resting state, we can selectively stimulate the inhibitory neuron by using a signal that only the inhibitory neuron is fast enough to respond; similarly, when the neurons are in an “inhibited” state (i.e. membrane potential lower than regular resting state and corresponding elevated  $h$  value), we can selectively stimulate the excitatory neuron by using a signal such that the quicker  $h$  of the inhibitory

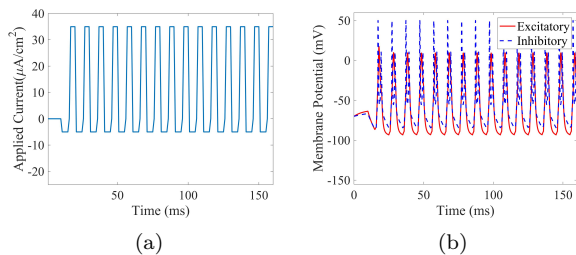


Fig. 3. An applied current waveform with a small dip followed by a large spike that stimulates excitatory and inhibitory neurons at 100 Hz. (a) Applied waveform (b) Resulting membrane potentials.

neuron would be fast enough to decrease in response to the input so inhibitory firing would not occur, while the slower  $h$  of the excitatory neuron would stay high enough to cause excitatory firing. These intuitions are used in Section III for tailoring waveforms to neuron-types.

### C. Estimating Firing Events

For the results detailed in this paper, neuron firing is characterized by a discontinuous jump in the amplitude of the response of the membrane potential. This discontinuous jump is identified at a point where a small increase in applied current waveform magnitude causes a significant, disproportionate increase in the amplitude of the response. Any response with amplitude beyond this discontinuous jump is considered to be characteristic of a neuron firing.

## III. RESULTS

For all the results below, we use periodic signals for simplicity, and we aim to achieve a firing rate of 100 Hz, which is experimentally achievable for mammalian neurons during stimulation [11].

### A. Non-Selective Signal

First we start with a signal that stimulates both neurons non-selectively. In order to achieve this, we choose each cycle of the signal to have a small dip of  $5 \mu A/cm^2$  amplitude and 5 ms width, followed by a large spike of  $35 \mu A/cm^2$  amplitude and 5 ms width, with a transition time of 1 ms. The short dip in the waveform increases  $h$  by decreasing the membrane potential, and the large spike in the waveform is large enough such that it greatly increases  $m$  before a significant decrease of  $h$ . As a result, both of the neurons fire. The waveform as well as the responses of the two neurons are shown in Fig. 3.

### B. Inhibitory-Selective Signal

We now choose a signal that selectively simulates only the inhibitory neuron. In each cycle, we have a 5 ms dip of  $5 \mu A/cm^2$ , and a 5 ms spike of  $10 \mu A/cm^2$ . The short dip in the waveform increases  $h$  by decreasing the membrane potential, and the small spike in the waveform slightly increases  $m$ . In response to this signal, the excitatory neuron exhibits only small changes due to

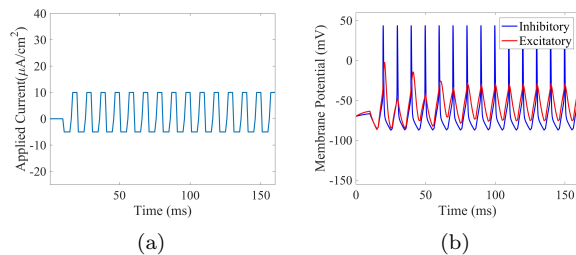


Fig. 4. An applied current waveform with a small dip followed by a small spike that stimulates only inhibitory and not excitatory neurons. The small spike is sufficient for only the faster inhibitory neuron to fire. (a) Applied waveform (b) Resulting membrane potentials.

the low amplitude of input and its slow dynamics. The behavior of the excitatory neuron does not meet the firing criteria specified in Section II-C. On the other hand, the inhibitory neuron has fast enough dynamics, such that the negative part of stimulation increases  $h$ , and the closely following positive part allows  $m$  to increase. The combination of increased  $m$  and high  $h$  allows the neuron to fire. The waveform for inhibitory-selective stimulation and the responses of the neurons are shown in Fig. 4.

### C. Excitatory-Selective Signal

Finally, in order to demonstrate bidirectional selective stimulation, we choose a signal that stimulates only the excitatory neuron. In each cycle of the signal, we have a 5 ms dip of  $22 \mu A/cm^2$ , and a 4 ms spike of  $20 \mu A/cm^2$ . In response to this applied current waveform, the inhibitory cortical cell type does not fire. First, the large dip in the waveform decreases  $m$  and increases  $h$  greatly by decreasing the membrane potential. Following that, the large spike in the waveform increases  $m$  in both neurons. In the inhibitory neuron, since  $m$  is starting from too low of a value due to the negative current phase, and  $h$  is fast enough to decrease, there is no point where both are high enough for the neuron to fire. As a result, the inhibitory neuron does not exhibit behavior that meets the firing criteria specified in Section II-C. However, the excitatory neuron does fire in response to this applied current waveform. This is because during the positive input,  $h$  remains high due to its slow dynamics, while the input is sufficient for  $m$  to increase. The input waveform as well as the resulting membrane potentials of the two neurons are shown in Fig. 5.

## IV. DISCUSSION

As the results have indicated, an understanding of the  $m$ ,  $n$ , and  $h$  plots can be used to tailor responses of two neuron-types bidirectionally. Specific applied current waveforms can be used to take advantage of variations in the time constants of  $m$ ,  $n$ , and  $h$  to cause differentiation in the response of neurons.

Though demonstrated on two specific neuron-types, this form of analysis can potentially be extended to tailor waveforms that produce selective stimulation between

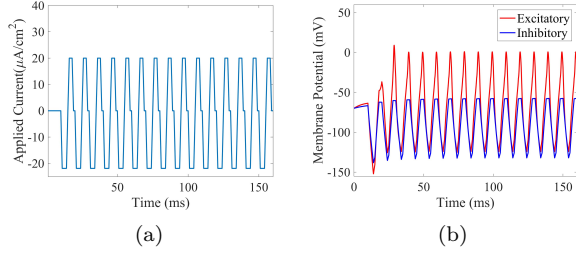


Fig. 5. An applied current waveform with a large dip followed by a large spike that stimulates only excitatory and not inhibitory neurons. Starting from the inhibited state, the large spike increases  $m$  in both neurons, but only the  $h$  in the slower excitatory neuron remains high enough. (a) Applied waveform (b) Resulting membrane potentials.

other neuron types with altered differential equations, given that the dynamics of the two neurons are different. More neuron-types will be considered in future work to explore the limits and limitations of our strategy.

However, when aiming to stimulate one neuron-type from a pool of more than two types of neurons, the  $m$ ,  $n$ , and  $h$  plots for the various neuron types would have to be analyzed pairwise to achieve satisfactory selective stimulation. The problem can scale quickly when more neuron-types are considered, so manual examination of  $m$ ,  $n$ , and  $h$  curves becomes impractical. Approaches involving computationally tuning the applied current waveforms may ameliorate this issue.

We use single neuron models to illustrate our stimulation strategies in this paper. In the brain, however, the neurons are interconnected to form networks, whose effects on the efficacy of selective stimulation is largely unknown. In future work, it is worth modeling the network effects on neuron-type selectivity, using network models such as those in [6].

Another limitation of the results of this study is that they have only been shown in a simulation context with waveforms applied to modified HH models. Experimental validation for the effectiveness of the tailored signals has not been acquired yet. In practice, neurons, even if of the same type, may receive altered signals due to neuron location or orientation, so other forms of signal design could further increase the stimulation selectivity.

## APPENDIX

The supplementary equations that are necessary for the differential equations of the excitatory neuron are as follows [8], [9]:

$$\begin{aligned}
 h_{\infty} &= \frac{1}{1 + e^{6.2(V+65)}} \\
 \alpha_m &= \frac{0.182(V+35)}{1 - e^{-(V+35)/9}}, \beta_m = \frac{-0.124(V+35)}{1 - e^{(V+35)/9}} \\
 \alpha_n &= \frac{0.02(V-20)}{1 - e^{-(V-20)/9}}, \beta_n = \frac{-0.002(V-20)}{1 - e^{(V-20)/9}} \\
 \alpha_h &= \frac{0.024(V+50)}{1 - e^{-(V+50)/5}}, \beta_h = \frac{-0.0091(V+75)}{1 - e^{(V+75)/5}}.
 \end{aligned}$$

TABLE I  
Constants used for the two neuron-types.

Parameter	Excitatory Neuron	Inhibitory Neuron
$C$ ( $\mu F/cm^2$ )	0.75	1
$\bar{g}_{Na}$ ( $mS/cm^2$ )	3	35
$\bar{g}_K$ ( $mS/cm^2$ )	10	9
$\bar{g}_L$ ( $mS/cm^2$ )	0.1	0.1
$E_{Na}$ (mV)	60	55
$E_K$ (mV)	-90	-90
$E_L$ (mV)	-60	-65

The supplementary equations that are necessary for the differential equations of the inhibitory neuron are as follows [10]:

$$\begin{aligned}
 \alpha_m &= \frac{0.1(V+35)}{1 - e^{-0.1(V+35)}}, \beta_m = 4e^{-(V+60)/18} \\
 \alpha_n &= \frac{0.01(V+34)}{1 - e^{-0.1(V+34)}}, \beta_n = 0.125e^{-(V+44)/80} \\
 \alpha_h &= 0.07e^{-(V+58)/20}, \beta_h = \frac{1}{1 + e^{-0.1(V+28)}}.
 \end{aligned}$$

The constants for each neuron type associated with these equations are summarized in Table I.

## References

- [1] N. Grossman, D. Bono, N. Dedic, S. B. Kodandaramaiah, A. Rudenko, H.-J. Suk, A. M. Cassara, E. Neufeld, N. Kuster, L.-H. Tsai, A. Pascual-Leone, and E. S. Boyden, "Noninvasive deep brain stimulation via temporally interfering electric fields," *Cell*, vol. 169, no. 6, pp. 1029–1041, 2017.
- [2] J. Cao and P. Grover, "STIMULUS: Noninvasive dynamic patterns of neurostimulation using spatio-temporal interference," *bioRxiv*, p. 216622, 2017.
- [3] D. K. Freeman, D. K. Eddington, J. F. Rizzo III, and S. I. Fried, "Selective activation of neuronal targets with sinusoidal electric stimulation," *Journal of neurophysiology*, vol. 104, no. 5, pp. 2778–2791, 2010.
- [4] M. Im and S. I. Fried, "Temporal properties of network-mediated responses to repetitive stimuli are dependent upon retinal ganglion cell type," *Journal of neural engineering*, vol. 13, no. 2, p. 025002, 2016.
- [5] P. Twyford, C. Cai, and S. Fried, "Differential responses to high-frequency electrical stimulation in on and off retinal ganglion cells," *Journal of neural engineering*, vol. 11, no. 2, p. 025001, 2014.
- [6] M. Mahmud and S. Vassanelli, "Differential modulation of excitatory and inhibitory neurons during periodic stimulation," *Frontiers in neuroscience*, vol. 10, p. 62, 2016.
- [7] Hodgkin, Alan L and Huxley, Andrew F, "A quantitative description of membrane current and its application to conduction and excitation in nerve," *The Journal of physiology*, vol. 15, no. 4, pp.500–544, 1952.
- [8] Z. F. Mainen, J. Joerges, J. R. Huguenard, and T. J. Sejnowski, "A model of spike initiation in neocortical pyramidal neurons," *Neuron*, vol. 15, no. 6, pp. 1427–1439, 1995.
- [9] R. D. Traub, R. K. Wong, R. Miles, and H. Michelson, "A model of a CA3 hippocampal pyramidal neuron incorporating voltage-clamp data on intrinsic conductances," *Journal of Neurophysiology*, vol. 66, no. 2, pp. 635–650, 1991.
- [10] X.-J. Wang and G. Buzsáki, "Gamma oscillation by synaptic inhibition in a hippocampal interneuronal network model," *Journal of neuroscience*, vol. 16, no. 20, pp. 6402–6413, 1996.
- [11] B. C. Carter and B. P. Bean, "Incomplete inactivation and rapid recovery of voltage-dependent sodium channels during high-frequency firing in cerebellar purkinje neurons," *Journal of neurophysiology*, vol. 105, no. 2, pp. 860–871, 2010.
- [12] F. Rattay, "Analysis of models for external stimulation of axons," *IEEE Trans Biomed Eng*, vol. 33, no. 10, pp. 974–977, 1986.